

# Dissolution Kinetics of a Copper Oxide Ore Sample and Optimizing the Effective Parameters, Using Response Surface Methodology

Rudarsko-geološko-naftni zbornik  
(The Mining-Geology-Petroleum Engineering Bulletin)  
UDC: 622-699  
DOI: 10.17794/rgn.2023.2.5

Original scientific paper



Hassan Maleki<sup>1</sup>; Sajjad Chehrehgani<sup>2</sup>; Mohammad Noaparast<sup>1</sup>; Mir Saleh Mirmohammadi<sup>1</sup>; Minoo Ghanbarzad<sup>1</sup>

<sup>1</sup> School of Mining Engineering, College of Engineering, University of Tehran, Tehran, Iran.

<sup>2</sup> Department of Mining Engineering, Urmia University, Urmia, Iran. ORCID (<https://orcid.org/0000-0003-4230-5454>).

## Abstract

In this research work, the leaching behavior of a copper oxide ore sample prepared from the Qaleh-Zari copper mine with a very high grade of 5.4% Cu (malachite and azurite) was investigated to evaluate the effects of significant operating parameters on copper recovery, including sulfuric acid concentration, solid percentage, particle size and agitation speed. Then, response surface methodology (RSM) and central composite design (CCD) were employed to optimize the leaching process and assess interactions between the effective parameters. In order to further analyze the leaching behavior, kinetics of copper dissolution was studied on the basis of the shrinking core models (SCM). The results showed a reduction in the rate of recovery with an increase in the solid percentage and/or particle size. In contrast, any increase in the agitation speed and/or acid concentration was found to improve the recovery. It was remarkable that increasing the sulfuric acid content, beyond a certain level, imposed no significant effect on the recovery. Optimal copper recovery was obtained with a solid percentage, agitation speed, particle size, and sulfuric acid concentration of 25.12%, 586 rpm, 70 μm, and 12.5%, respectively, leading to a recovery of 93.24%. A study on the leaching kinetics indicated that the dissolution rate was controlled by the fluid diffusion from product layer model with 30.71 kJ/mol of activation energy.

## Keywords:

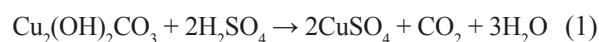
copper oxide; leaching, kinetics; response surface methodology; optimization

## 1. Introduction

Due to its excellent ductility, resistance to corrosion, thermal conductivity, and other useful properties, copper has found many applications in the construction industry, machinery manufacturing, power applications, and light industries, among others. Currently, the limited reserves of copper are unequally distributed around the world, which could significantly constrain the global economic development. Reasonable exploitation of the global copper reserves has long been a difficult challenge for balanced improvements of the world economy. With the drop in sulfidic mineral resources, the development and exploitation of copper oxide ore has been increasingly regarded to address the gap between the demand for and supply of copper (Han et al., 2021). In nature, copper is dominantly found in the form of sulfidic and oxidized minerals types, such as malachite, azurite, tenorite, bornite, chalcopyrite, chrysocolla, etc. (Deng et al., 2017; Naguman, 2008). Copper oxide processing has been practiced through three different methods. These include flotation (Feng et al., 2017, 2018), leaching (Rucher et al., 2017), and benefici-

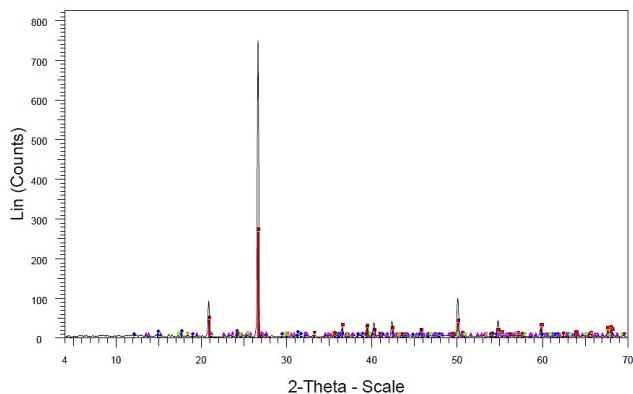
ation-metallurgy combination processes (Han et al., 2017). The flotation can be performed via either of two approaches, namely i) direct flotation, and ii) sulfidation-xanthate flotation (Deng et al., 2017). The second methodology, leaching, is the most common approach among these three processes. It includes a chemical reaction between the copper oxide and a leaching agent. Two classes of leaching have been distinguished, which are acid leaching and ammonia leaching (Haghighi et al., 2013; Turan, 2015). The third methodology refers to metallurgy combination processes which are increasingly regarded, particularly in the recent past years (Bia et al., 2018).

Today, sulfuric acid is acknowledged as the most efficient leaching agent for copper oxide ore. The dissolution of malachite (Cu<sub>2</sub>(OH)<sub>2</sub>CO<sub>3</sub>), as a copper oxide mineral, in sulfuric acid can be addressed as follows:



The dissolution of sulfide and oxide minerals is significant in a broad spectrum of different fields, including mineral processing, geochemistry, hydrometallurgy, and material science. The knowledge of the dissolution mechanism would be contributed to better design and optimization of copper exploitation processes (Crundwell, 2014). In this respect, much attention has been paid to the studies

Corresponding author: Sajjad Chehrehgani  
e-mail address: s.chehrehgani@urmia.ac.ir



Type: 2Th/Th locked - Start: 4.000° - End: 70.000 - Step: 0.020- Operations: Smooth 0.150 | Background 1.000,1.000 | Import

- 46-1045(\*) - Quartz, syn -  $\text{SiO}_2$ -S-Q 84.6% - Hexagonal - Y: 25.83 % - d x by: 1.- WL:
- ◆ 41-1390 (1) - Malachite, syn -  $\text{Cu}_2(\text{CO}_3)(\text{OH})_2$  - S-Q 6.1 % - Monoclinic - Y: 0.88 % - d x
- ▲ 31-0966 (\*) - Orthoclase - KAISI3O8-S-Q 3.7 % - Monoclinic - Y: 0.33 % - d x by: 1. - W
- 01-0564 (D) - Azurite -  $2\text{CuCO}_3 \cdot \text{Cu}(\text{OH})_2$ -S-Q 3.1 % - Monoclinic - Y: 0.28% - d x by: 1
- ▼ 13-0534 (D) - Hematite, syn -  $\text{Fe}_2\text{O}_3$  - S-Q 1.4 % - Rhombohedral - Y: 0.33 % - d x by: 1.
- ⊠ 19-0629 (\*) - Magnetite, syn -  $\text{FeFe}_2\text{O}_4$  - S-Q 1.0 % - Cubic - Y: 0.43 % - d x by: 1. - WL:

Figure 1: Peaks of XRD spectrum

Table 1: Composition of ore sample

Composition or element	%	Composition or element	%
$\text{SiO}_2$	80.79	MnO	<0.05
$\text{Al}_2\text{O}_3$	2.40	$\text{Na}_2\text{O}$	0.07
BaO	<0.05	$\text{P}_2\text{O}_5$	<0.05
CaO	0.16	$\text{SO}_3$	0.52
$\text{Fe}_2\text{O}_3$	5.94	$\text{TiO}_2$	0.05
$\text{K}_2\text{O}$	0.28	Cu	5.84
MgO	0.14	LOI	3.67

on the copper dissolution behavior and kinetics. Several researchers have investigated the dissolution behavior and kinetics of copper oxide ore using various solvents. These included mineral acids like HCl,  $\text{H}_2\text{SO}_4$ , and  $\text{HNO}_3$  (Bingöl and Canbazoglu, 2004; Ata et al., 2001; Shayestehfar et al., 2008; Habbache et al., 2009), organic acids like citric acid and lactic acid (Habbache et al., 2009; Shabani et al., 2014; Deng et al., 2015), chlorine (Ekmekyapars et al., 1988), ammonium hydroxide or ammonium salts like ammonium chloride, ammonium nitrate, ammonium sulfate, ammonium acetate, ammonium citrate, etc. (Wei et al., 2010; Ekmekyapar et al., 2012; Künkül et al., 2013; Wu et al., 2013; Ekmekyapar et al., 2015; Mao et al., 2016), and alkaline solutions of glycine (Tanda et al., 2017).

In order to better manage the experiments, response surface methodology (RSM) is employed in this re-

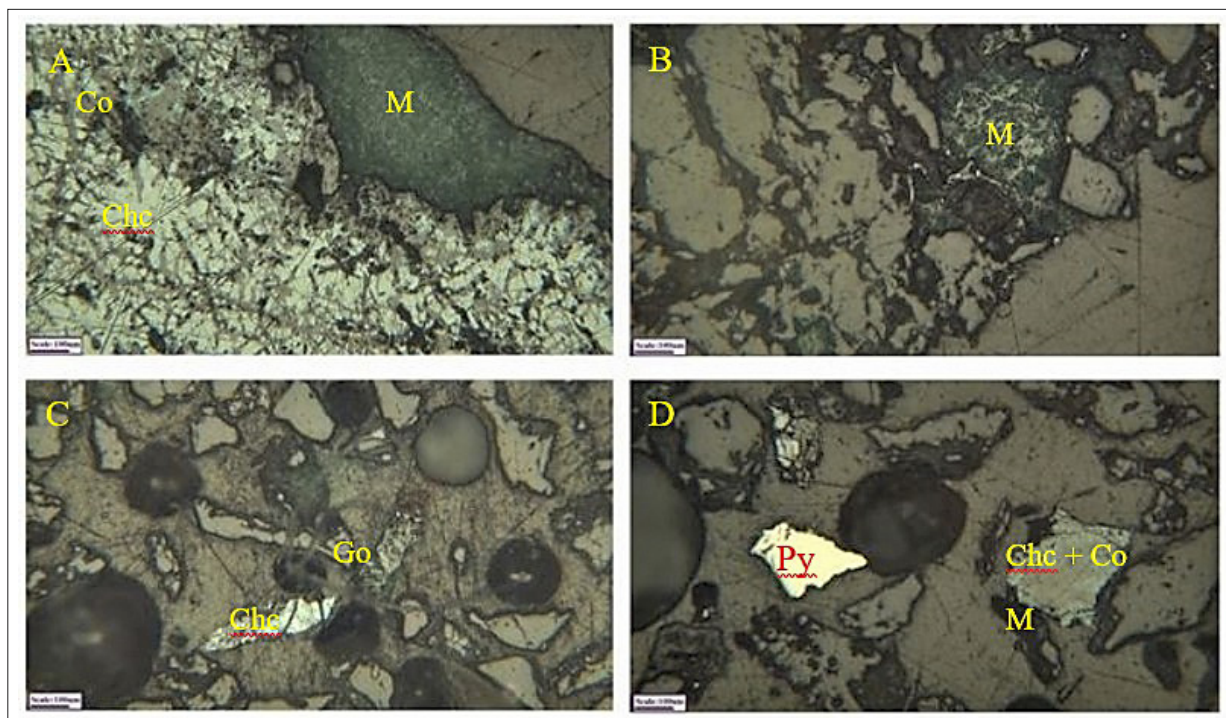


Figure 2: A) a sample containing chalcocite (Chc), covellite (Co), and entrained malachite (M), B) malachite entrained with nonmetallic gangue, C) malachite entrained with chalcocite and goethite (Go), D) a sample containing pyrite (Py), malachite, and remained chalcocite and covellite.

search work. The implementation of RSM requires the use of a rational empirical design method upon acquiring the required data through actual experiments. Subsequently, quadratic multivariate regression equations are used to fit a function to the relationship between tested parameters and the response. Furthermore, a stochastic method has been developed to analyze the regression model and then optimally parameterize the process. The number of required experiments is relatively small using this methodology which saves time and raw material as well. Central composite design (CCD) is a common method of response surface analysis which is frequently used for examining nonlinear effects of factors, test condition optimization to minimize material consumption, and inter-factor association analysis (Bia et al., 2018).

An accurate understanding of the dissolution kinetics allows for interpreting a naturally complex leaching behavior. Thus, this research is aimed to investigate and discuss the leaching kinetics and parameters of dissolution of copper oxide ore using sulfuric acid. Here we study the dissolution kinetics based on the shrinking core model (SCM), with the best kinetic model for describing the leaching process of copper oxide ore which is further introduced. In addition, DX13 software was utilized to optimize the parameters affecting the copper dissolution from the copper oxide ore by sulfuric acid.

Although many researches have been performed to gain a better understanding of the leaching process and its operation, the modeling approach using statistical information with the aim of optimizing the process combined with kinetic analysis can be a new prospect in research related to the acidic dissolution of copper oxide ore..

## 2. Materials and methods

### 2.1. Materials

The copper oxide ore sample that was studied in this research was from the Qaleh-Zari copper mine in Birjand, southeast of Iran. After two stages of crushing (by jaw and roll crushers) and milling (by ball mill), the prepared sample was subjected to X-ray diffraction (XRD) analysis to characterize the composition of the copper oxide minerals. **Figure 1** demonstrates the peaks observed upon the XRD analysis. The copper content of the ore sample was in the form of malachite ( $\text{Cu}_2(\text{OH})_2\text{CO}_3$ ) and azurite ( $\text{CuCO}_3\text{Cu}(\text{OH})_2$ ). The rest of the ore was found to be composed of quartz ( $\text{SiO}_2$ ), alkyl feldspar ( $\text{KAlSi}_3\text{O}_8$ ), hematite ( $\text{Fe}_2\text{O}_3$ ), and magnetite ( $\text{Fe}_3\text{O}_4$ ).

In order to conduct an elemental analysis on the sample, X-ray fluorescence (XRF) analysis was further employed. Based on the results, the sample contained 5.84% of copper, with Si, Al, and Fe being the main impurities. **Table 1** depicts the ore sample composition.

Mineralogical studies showed that the -160+75 microns size fraction contained malachite at 10-13 vol.%,

iron oxide-hydroxide including goethite-limonite and hematite at a total of 5-7 vol.%, and chalcocite at 0.5-1 vol.%. The degree of liberation (DOL) in above mentioned size fraction was evaluated to be about 75–80% for malachite and 80–85% for chalcocite-covellite. The chalcocite was observed to be entrained by nonmetallic gangue and malachite. In this size fraction (-160+75 microns), some intact pieces of amorphous pyrite were also observed (see **Figure 2**).

### 2.2. Methodology

To run the leaching tests, 500 g of sample was used in each test. First, pulp with a predetermined solid percentage, was loaded into a flask. Then, a specified amount of sulfuric acid at a certain concentration was further added to the flask. Adjusting the agitation speed for a 2 h at room temperature, the mixture was then filtered, dried, and weighed. The leach solution was stirred by mechanical stirrer with a Teflon-lined impeller. In the experiment, the four main condition variables (factors) that affect the leaching process (solid percentage, agitation speed, particle size and acid concentration) were selected. The solution and residual solid were collected and copper grade was measured using atomic absorption technique. The following equation was used to calculate copper recovery upon the leaching process:

$$R_{Cu} = \frac{C * V}{Ff} \times 100 \quad (2)$$

where:

- C: post-leaching concentration of metal ion in the solution in g/L,
- V: leaching solution volume in L,
- F: feed weight in g,
- f: feed grade in percentage.

In experiments, four major parameters affecting the leaching process (solid percentage, agitation speed, particle size, and sulfuric acid concentration) were selected on the basis of the CCD. The tests were then analyzed with the help of RSM in DX13 software.

### 2.3. Leaching kinetics

Leaching process is a heterogeneous reaction that includes ionic reactants and mass transfer. When a substance exhibits low solubility, it can be dissolved through a chemical process in which gradual shrinkage of core particle and thickening of the dissolution layer occur. By increasing the dissolution time, the particle shrinks to a point where the entire particle shell is dissolved. This process can be determined by the SCM, if a layer is formed during the process, and shrinking particle model (SPM) otherwise. Reaction rate can be defined by diffusion from a fluid layer model, diffusion from a product layer model, a surface chemical reaction model, or a hybrid of them. In the SCM, the reaction is assumed to start from the outer shell of the solid particle and proceed in-



ward to a point where the solid material is completely transformed, leaving some neutral residual solid (Abdi, 2015). Based on this model, the dissolution process can be described by one of the following Equations 3-6 (Agacayak et al., 2017). A new model, based on the interface transfer and diffusion through the product layer was applied to explain the malachite leaching. This model is given as follows in Equation 7 (Abdelraheem et al., 2022; D. Bingol et al., 2005).

If the leaching process is controlled by the fluid film diffusion, then:

$$1 - (1-x)^{2/3} = kt \tag{3}$$

and if the leaching process is controlled by the fluid diffusion from the product layer, then:

$$1 - 3(1-x)^{2/3} + 2(1-x) = kt \tag{4}$$

If the reaction progress is controlled by a surface chemical reaction, then:

$$1 - (1-x)^{1/3} = kt \tag{5}$$

Both diffusion and chemical mixture model:

$$1 - 2(1-x)^{2/3} + (1-x)^{1/3} = kt \tag{6}$$

Mixed model based on the interface transfer and diffusion through the product layer:

$$(1/3)LN(1-x) - [1 - (1-x)^{1/3}] = kt \tag{7}$$

where:

- X: fraction reacting with the leaching agent for a pre-determined reaction time,
- k: reaction rate constant in 1/min,
- t: time in min.

Figures 3 to 7 show the results of model fitting to the obtained experimental data.

In the presented plots, the slope of each fitted line indicates its relevant reaction rate. Moreover, the rate-controlling model is the one that produces the highest correlation coefficient. As the results indicate, the highest correlation coefficient is the one for fluid diffusion from product layer model.

In the leaching process, the dissolution rate depends on the activation energy which can be calculated by the

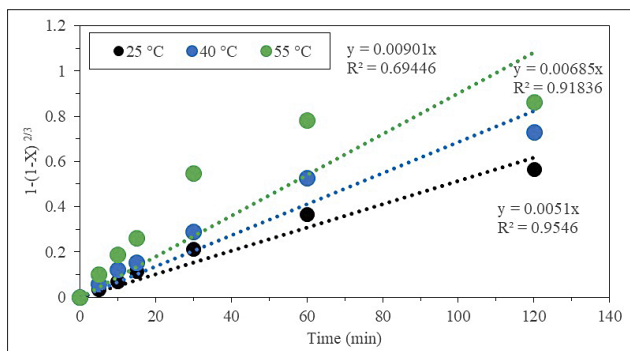


Figure 3: Results of fitting the liquid film diffusion model to experimental data.

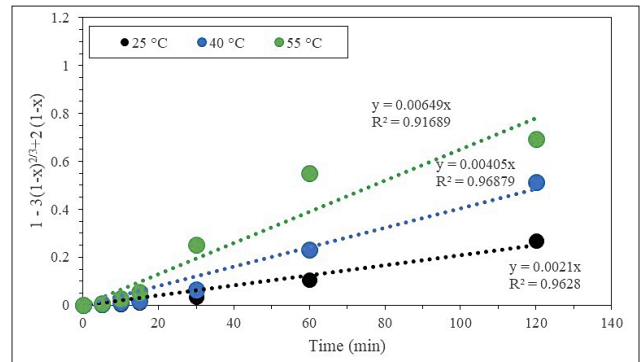


Figure 4: Results of fitting the fluid diffusion from product layer model to experimental data.

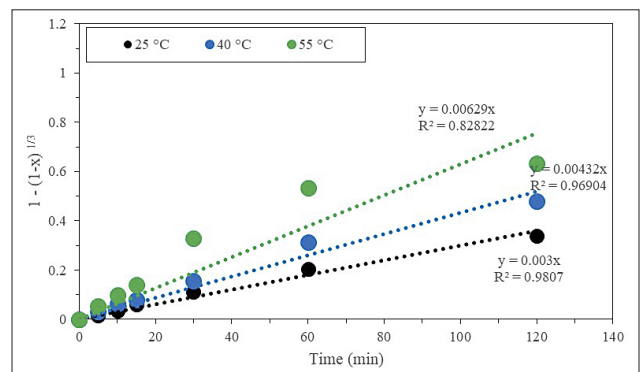


Figure 5: Results of fitting the surface reaction model to experimental data.

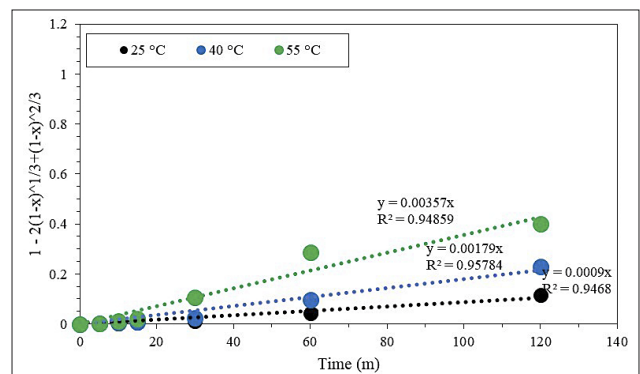


Figure 6: Results of fitting the both diffusion and chemical mixture model to experimental data.

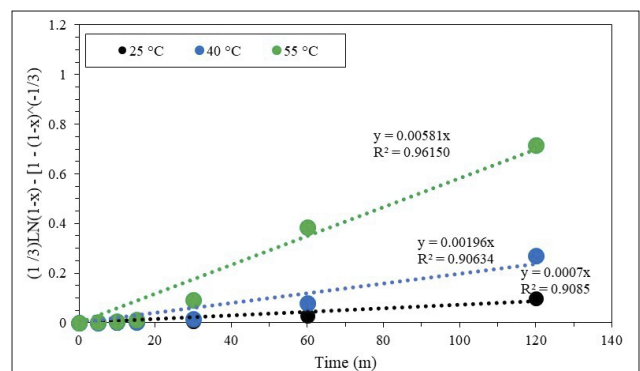
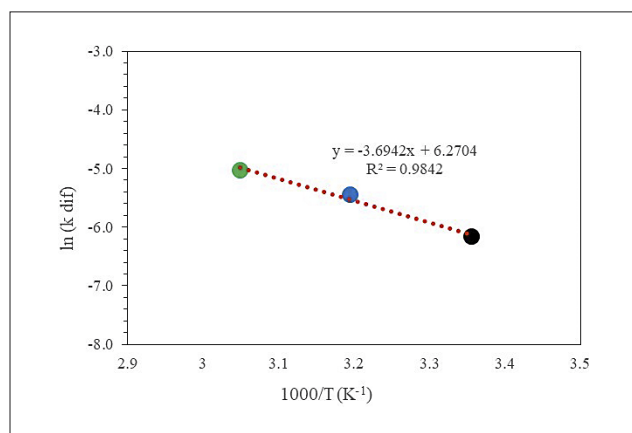


Figure 7: Results of fitting the mixed model based on the interface transfer and diffusion through the product layer to experimental data.

Arrhenius equation. Therefore, activation energy was herein taken as the rate-controlling factor for the leaching reaction.



**Figure 8:** Arrhenius diagram based on the fluid diffusion from product layer model.

#### 2.4. Activation energy

Association of the reaction rate constant with temperature can be quantified by the Arrhenius equation, as follows (Apua et al., 2021):

$$K = A \times e^{\frac{-E_a}{R \times T}} \quad (8)$$

where:

- K: reaction rate constant in 1/min,
- A: frequency factor in 1/min,
- E<sub>a</sub>: activation energy of reaction (J/mol),
- R: universal gas constant (8.314 kJ/mol),
- T: temperature in K.

Based on the fluid diffusion from product layer model, the Arrhenius equation plot in the form of Ln(K) versus 1/T for the leaching process at different temperatures was presented in **Figure 8**. Knowing that the slope of the fitted line to this plot is equal to  $-E_a/R$ , the activation energy was then calculated.

**Table 2:** Parameters and relevant levels

Factor Name	Minimum	Coded Low	Mean	Coded High	Maximum
A: solid percentage	20	25	30	35	40
B: agitation speed (rpm)	300	400	500	600	700
C: particle size (μm)	53	70	90	106	150
D: acid concentration %	5	10	15	20	25

**Table 3:** Results and conditions of designed tests

St.d.	Run	Solid percentage	Agitation speed (rpm)	Particle size (μm)	Acid concentration %	Recovery %
13	1	30	500	53	15	93.22
19	2	30	500	90	15	82.56
11	3	30	300	90	15	74.67
3	4	35	400	106	20	75.43
21	5	30	500	90	15	82.98
4	6	25	600	70	20	89.27
17	7	30	500	90	15	81.79
16	8	30	500	90	25	81.94
5	9	35	400	70	20	83.9
1	10	35	600	106	10	72.71
15	11	30	500	90	5	68.64
20	12	30	500	90	15	82.68
10	13	40	500	90	15	74.12
14	14	30	500	150	15	67.39
2	15	35	600	70	10	84.39
8	16	25	400	70	10	84.85
6	17	25	400	106	10	70.87
7	18	25	600	106	20	73.34
12	19	30	700	90	15	87.63
9	20	20	500	90	15	86.53
18	21	30	500	90	15	83.1

In general, the activation energy for a chemically controlled mechanism is greater than 40 kJ/mol, while the activation energy for a diffusion-controlled mechanism is less than 40 kJ/mol (Ekmekyapar et al., 2012 ; Espirari et al., 2006) and if the activation energy is less than 20 kJ/mol, the penetration of the fluid film diffusion is the controlling rate of leaching (Yoshida, 2003). The mentioned methodology led to the activation energy of 30.71 kJ/mol which is lower than 40 and higher than 20 kJ/mol. The obtained value of activation energy indicated that the leaching process rate is controlled by the fluid diffusion from product layer model.

### 3. Design and analysis of leaching process with DX13 software

#### 3.1. Parameters and results of designed tests

In order to model and optimize the parameters affecting the leaching of copper oxide by sulfuric acid, particle size, agitation speed, solid percentage, and acid concentration (wt./wt.%) were selected as the variable parameters. Washing time and temperature are the pa-

rameters that were kept constant. **Table 2** presents a list of the effective parameters and their studied levels.

Results and conditions of the conducted tests are given in **Table 3**.

#### 3.2. Analysis of variance

Focusing on the leaching of copper oxide minerals, analysis of variance (ANOVA) shows the significance of the model and the most effective parameters in terms of the significance of their impacts on the response. In fact, ANOVA refers to a series of mathematical operations that are used to figure out whether or not average inter-group differences are significant. In these experiments, quadratic model was selected in the software, and the ANOVA which was presented by software is given in **Table 4**.

According to **Table 4**, the F-value was found to be 349.09, which indicates the model significance, so that the probability of noise-induced significance of F is as low as 0.01%. The value of fitting error (0.35) shows that the error is not significant with respect to total error. The probability that such a high F-value of fitting error

**Table 4:** Details of ANOVA model

Source	Sum of Squares	Df	Mean Square	F-value	P-value	
<b>Model</b>	1010.11	14	72.15	349.09	<0.0001	significant
<b>A</b>	77.00	1	77.00	372.57	<0.0001	
<b>B</b>	83.98	1	83.98	406.32	<0.0001	
<b>C</b>	646.48	1	646.48	3128.86	<0.0001	
<b>D</b>	88.44	1	88.44	428.92	<0.0001	
<b>AB</b>	19.10	1	19.10	92.40	<0.0001	
<b>AC</b>	11.91	1	11.91	57.61	0.0003	
<b>AD</b>	28.25	1	28.25	136.68	<0.0001	
<b>BC</b>	3.33	1	3.33	16.10	0.0070	
<b>BD</b>	32.83	1	32.83	158/86	<0.0001	
<b>CD</b>	0.1984	1	0.1984	0.9602	0.3650	
<b>A2</b>	8.00	1	8.00	38.70	0.0008	
<b>B2</b>	3.22	1	3.22	15.59	0.0076	
<b>C2</b>	8.14	1	8.14	39.39	0.0008	
<b>D2</b>	83.44	1	83.44	403.70	<0.0001	
<b>Residual</b>	1.24	6	0.2067			
<b>Lack of Fit</b>	0.1840	2	0.0920	0.3485	0.7252	not significant
<b>Pure Error</b>	1.06	4	0.2640			
<b>Cor Total</b>	1011.35	20				

**Table 5:** Results of statistical evaluations

<b>St.d. Dev.</b>	0.4546	<b>R<sup>2</sup></b>	0.99
<b>Mean</b>	80.20	<b>Adjusted R<sup>2</sup></b>	0.99
<b>C.V.%</b>	0.56	<b>Predicted R<sup>2</sup></b>	0.98
		<b>Adeq Precision</b>	66.18

occurs due to noise which was estimated at 72.52%. **Table 5** presents the results of statistical evaluations.

**Table 5** presents the predicted R<sup>2</sup> that is proportional to adjusted R<sup>2</sup> and their difference is below 0.2. It is clear that Adeq precision measures the signal-to-noise ratio (SNR), and SNR values above 4 are desirable.

However, **Table 5** reports that SNR is 66.18 in this study, which is well acceptable. In **Table 5**, C.V. denotes the coefficient of variance, and it should be noted that lower values are desirable. Finally, the mathematical model for the copper recovery which was calculated by software from the coded factors is as follows:

$$\begin{aligned} \text{Cu Recovery} = & +82.62 - 3.10 \times A + 3.24 \times B - 6.36 \times C + \\ & + 3.33 \times D + 2.31 \times AB + 1.22 \times AC + 2.66 \times AD - \\ & - 0.6450 \times BC - 2.86 \times BD + 0.1575 \times CD - 0.5646 \times \\ & \times A^2 - 0.3583 \times B^2 - 0.5696 \times C^2 - 1.82 \times D^2 \quad (9) \end{aligned}$$

### 3.3. Model validation

#### 3.3.1. Plot of actual response versus predicted response

This plot is normally used to identify the value(s) that cannot be simply predicted by the model. **Figure 9** shows the plot of actual response versus predicted response. The fact that the predicted value is closer to the actual value implies that **Equation 9** is accurate and acceptable.

#### 3.3.2. Box-Cox plot

Box-Cox plot is presented in **Figure 10**. With this plot, the order of the model is controlled. In cases where the system has a non-normal distribution, response transformation using mathematical operators is used. Considering the appropriateness of the order of the model, and that the lambda obtained does not go out of the specified confidence range, no transfer was required.

### 3.4. Parameter interactions

**Figures 11 to 13** show the effects of the interaction of solid percentage with agitation speed, particle size, and acid concentration, respectively. In all figures, copper recovery decreases with a solid percentage increase. It stems from the fact that with a decrease in the solid percentage, the available acid for each particle increases, and the copper recovery accordingly increases, while the suspension and viscosity of the system decreases.

Based on the results shown in **Figure 11** the copper recoveries increase with an agitation speed increase for all solid percentages. In fact, a higher agitation speed boosts the mixing rate while lowering the resistance of the boundary layer against mass transfer. Therefore, the acid diffusion from the solution into the solid particles increases, and the copper dissolution out of the copper oxide minerals accordingly increases (**Azizi et al., 2018**). At a higher solid percentage, the increase in recovery with an increase in the agitation speed was observed to be steeper, so that the highest recovery was obtained at a low solid percentage coupled with a high agitation speed.

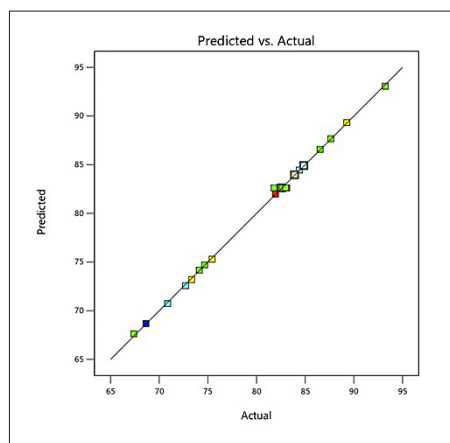


**Figure 9:** Plot of actual response versus predicted response.

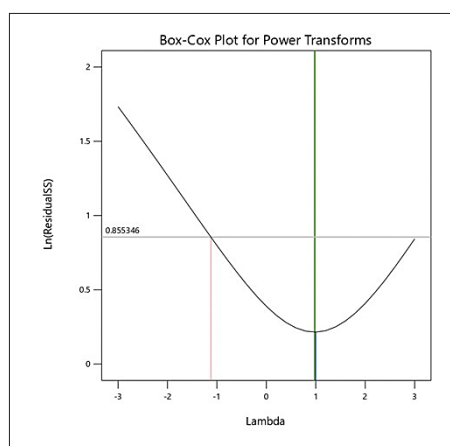


**Figure 10:** Box-Cox plot.

With a higher solid percentage and particle size, the recovery was lowered abruptly. This reduction is postulated from the presence of low-DOL coarse particles that could not be mixed properly, as seen in **Figure 12**.

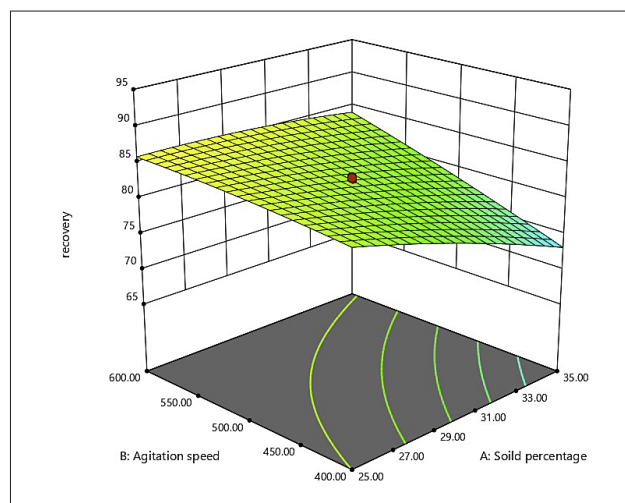


**Figure 11:** Three-dimensional plot of variations of copper recovery versus solid percentage and agitation speed at constant particle size and acid concentration of 90  $\mu\text{m}$  and 15%, respectively.



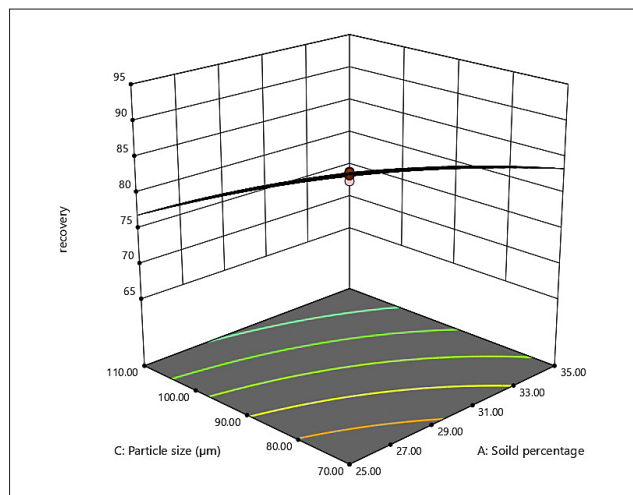


**Figure 12:** Three-dimensional plot of variations of copper recovery versus solid percentage and particle size at constant stirring and acid concentration of 500 rpm and 15%, respectively.

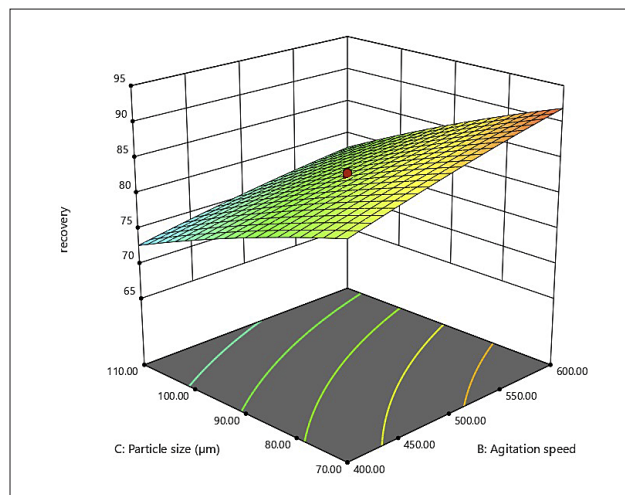


**Figure 14:** Three-dimensional plot of variations of copper recovery versus particle and agitation speed at constant solid percentage and acid concentration of 30% and 15%, respectively.

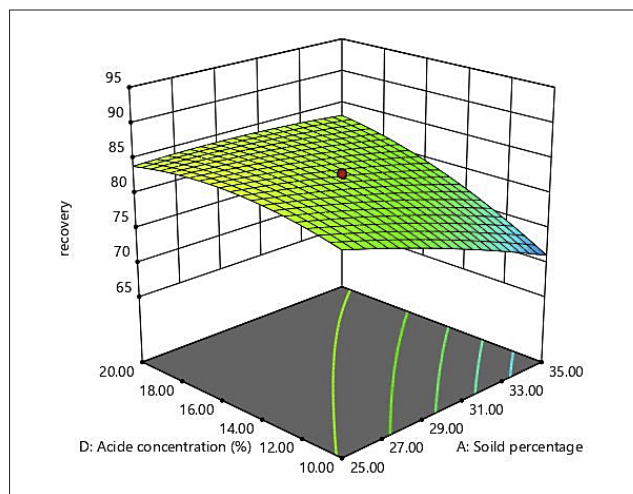


**Figure 13:** Three-dimensional plot of variations of copper recovery versus solid percentage and acid concentration at constant particle size and agitation speed of 90  $\mu\text{m}$  and 500 rpm, respectively.

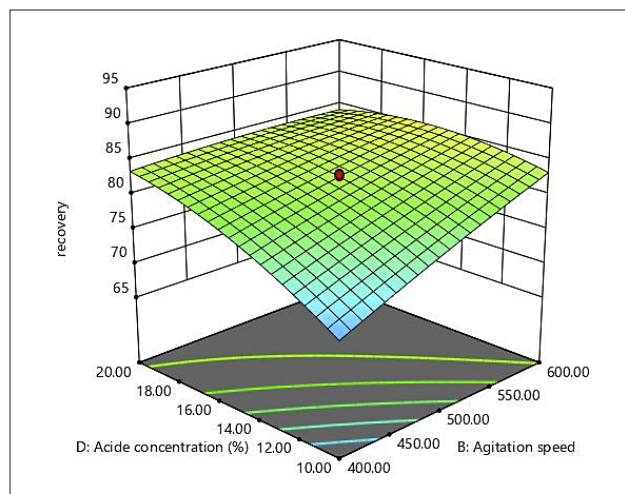


**Figure 15:** Three-dimensional plot of variations of copper recovery versus acid concentration and agitation speed at constant particle size and solid percentage of 90  $\mu\text{m}$  and 30%, respectively.

**Figure 13** indicates that, at lower acid concentrations, the copper recovery decreases with a higher solid percentage, while the decrease in recovery is smaller at higher acid concentrations. In general, the recovery increases with an increase in the acid concentration. Wang's work confirms this (Wang et al., 2019).

According to **Figure 14**, in all dimensions, the recovery increases with a higher agitation speed, and the maximum agitation speed occurred at maximum agitation speed coupled with minimum particle size. The interaction of these two parameters is in such a way that a decrease in particle size and an increase in agitation speed would improve the recovery.

The interaction of acid concentration with the agitation speed is demonstrated in **Figure 15**, where the recovery decreases when the acid concentration and agitation speed

get lower simultaneously. An increase in the agitation speed tends to accelerate the material dissolution. Agacayak et al., reported that the dissolution increased as the agitation speed increased (Agacayak et al., 2017).

As shown in **Figure 16**, the interaction of particle size and acid concentration is so that the recovery increases with the acid concentration regardless of the particle size. Maximum recovery was with minimum particle size and maximum acid concentration. However, finer particles exhibit a desirable DOL and a larger contact area with the acid (Liu et al., 2016; Li et al., 2017).

### 3.5. Optimization of leaching conditions

Numerical optimization of test conditions for achieving the maximum recovery is among the most important



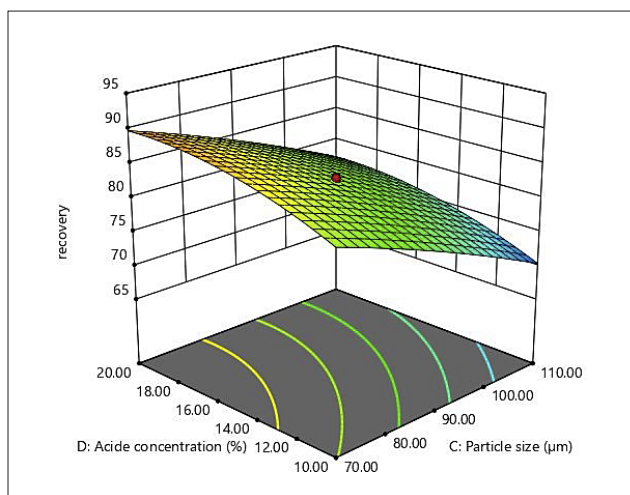


**Figure 16:** Three-dimensional plot of variations of copper recovery versus particle size and acid concentration at constant solid percentage and agitation speed of 30% and 500 rpm, respectively.

agent. For -70  $\mu\text{m}$  sample, acid consumption was estimated at 107 kg/t of copper oxide ore. The kinetics of the leaching of copper out of the oxidized mineral was studied using the SCM. The fluid diffusion model exhibited the highest correlation coefficient when fitted to the experimental data, indicating that the fluid diffusion model controls the rate of copper dissolution in sulfuric acid. Activation energy was obtained as 30.71 kJ/mol. Response surface methodology (RSM) and central composite design (CCD) were employed to optimize the leaching process and assess interactions between the effective parameters. The response surface methodology is an effective method to optimize experiment conditions and achieve an ideal experiment result. Among the studied parameters, solid percentage, agitation speed, particle size, and acid concentration were the effective parameters.

The results showed that the recovery decreases with an increase in the solid percentage and particle size. On

**Table 6:** Optimization conditions and relevant results

No.	Response	Goal	Solid percentage	Agitation speed (rpm)	Particle size ( $\mu\text{m}$ )	Acid concentration %	Recovery %
1	Recovery	Maximum	25.1	586	70	12.5	93.24

**Table 7:** Results of validation of the optimal conditions

Test No.	Solid percentage	Agitation speed (rpm)	Particle size ( $\mu\text{m}$ )	Acid concentration %	Recovery %
1	25.1	586	70	12.5	92.47
2	25.1	586	70	12.5	91.98

objectives of the design of experiment approach. Upon this task, the parameters are set to the levels that lead to the most desirable test results. **Table 6** presents the results of optimization.

In order to validate the results, two tests were performed under optimal conditions. The results of these tests were acceptably in agreement with the software predictions, as presented in **Table 7**.

#### 4. Conclusion

In this research work, the copper oxide ore sample from the Qaleh-Zari Mine was used in leaching tests using sulfuric acid under various conditions. The following conclusions were drawn upon studies the analysis results: based on mineralogical studies and chemical analyses on the initial sample, it was revealed that the copper oxide was dominantly composed of malachite and azurite minerals.

Given that most of the copper content of the ore was sourced from carbonate minerals (i.e. malachite and azurite), sulfuric acid was the best choice as a leaching

the other hand, increased agitation speed and/or acid concentration tend to improve the copper recovery. This was while the increase in sulfuric acid beyond a certain level, shows no significant effects to improve the recovery. Optimal values of the studied parameters were found to be a solid percentage, agitation speed, particle size, and acid concentration of 25.12%, 586 rpm, 70  $\mu\text{m}$ , and 12.5%, respectively, leading to a recovery of 93.24%.

#### 5. References

- Abdelraheem, MTO, Agacayak, T., (2022): Effect of organic and inorganic compounds on dissolution kinetics of chalcopyrite in hydrogen peroxide–Hydrochloric acid system. *Journal of Saudi Chemical Society* 26 (3), 101478. <https://doi.org/10.1016/j.jscs.2022.101478>.
- Abdi B. (2015): Investigation of dissolution kinetics of oxidized copper ore in alkaline media. A thesis presented for the degree of Master of Science in Tarbiat Modares University.
- Agacayak, T and Aras, A., (2017): Dissolution Kinetics of Nickel from Gordes (Manisa-Turkey) Lateritic Ore by Sul-

- phuric Acid Leaching under Effect of Sodium Fluoride, Selcuk University Journal of Engineering, Science and Technology, 5(3), pp: 353 – 361. <https://doi.org/10.1252/jcej.13we035>.
- Apua MC, Madiba MS. (2021): Leaching kinetics and predictive models for elements extraction from copper oxide ore in sulphuric acid. Journal of the Taiwan Institute of Chemical Engineers. 1;121:313-20. <https://doi.org/10.1016/j.jtice.2021.04.005>.
- Ata ON, Çolak S, Ekinci Z, Çopur M. (2001): Determination of the optimum conditions for leaching of malachite ore in H<sub>2</sub>SO<sub>4</sub> solutions. Chemical Engineering & Technology: Industrial Chemistry-Plant Equipment-Process Engineering-Biotechnology. 24(4):409-13. [https://doi.org/10.1002/1521-4125\(200104\)24:4%3C409::AID-CEAT409%3E3.0.CO;2-0](https://doi.org/10.1002/1521-4125(200104)24:4%3C409::AID-CEAT409%3E3.0.CO;2-0).
- Azizi A, Bayati B, Karamoozian M. (2018): A comprehensive study of the leaching behavior and dissolution kinetics of copper oxide ore in sulfuric acid lixiviant. Scientia Iranica. 1;25(3):1412-22. <https://doi.org/10.24200/sci.2018.5226.1154>.
- Bai X, Wen S, Liu J, Lin Y. (2018): Response surface methodology for optimization of copper leaching from refractory flotation tailings. Minerals. 18;8(4):165. <https://doi.org/10.3390/min8040165>.
- Bingöl D, Canbazoglu M. (2004): Dissolution kinetics of malachite in sulphuric acid. Hydrometallurgy. 1;72(1-2):159-65. <https://doi.org/10.1016/j.hydromet.2003.10.002>.
- Crundwell FK. (2014): The mechanism of dissolution of minerals in acidic and alkaline solutions: Part III. Application to oxide, hydroxide and sulfide minerals. Hydrometallurgy. 1;149:71-81. <https://doi.org/10.1016/j.hydromet.2014.06.008>.
- D. Bingol, M. Canbazoglu, S. Aydogan, (2005): Dissolution kinetics of malachite in ammonia/ammonium carbonate leaching, Hydrometallurgy, 76 (1–2), pp. 55-62, <https://doi.org/10.1016/j.hydromet.2004.09.006>.
- Deng J, Wen S, Deng J, Wu D, Yang J. (2015): Extracting copper by lactic acid from copper oxide ore and dissolution kinetics. Journal of Chemical Engineering of Japan. 20; 48(7):538-44. <https://doi.org/10.1252/jcej.14we032>.
- Deng J, Wen S, Yin Q, Wu D, Sun Q. (2017): Leaching of malachite using 5-sulfosalicylic acid. Journal of the Taiwan Institute of Chemical Engineers. 1;71:20-7. <https://doi.org/10.1016/j.jtice.2016.11.013>.
- Deng, D.; Xu, L.H.; Tian, J.; Hu, Y.H.; Han, Y.X. (2017): Flotation and Adsorption of a New Polysaccharide Depressant on Pyrite and Talc in the Presence of a Pre-Adsorbed Xanthate Collector. Minerals, 7, 40. <https://doi.org/10.3390/min7030040>.
- Ekmekyapar A, Aktaş E, Künkül A, Demirkiran N. (2012): Investigation of leaching kinetics of copper from malachite ore in ammonium nitrate solutions. Metallurgical and Materials Transactions B. 43(4):764-72. <https://doi.org/10.1007/s11663-012-9670-2>.
- Ekmekyapar A, Demirkiran N, Künkül AS, Aktaş E. (2015): Leaching of malachite ore in ammonium sulfate solutions and production of copper oxide. Brazilian Journal of Chemical Engineering. 32:155-65. <https://doi.org/10.1590/0104-6632.20150321s00003211>.
- Ekmekyapars A, Clolak S, Alkan M, Kayadeniz I. (1988): Dissolution kinetics of an oxidized copper ore in water saturated by chlorine. Journal of Chemical Technology & Biotechnology. 43(3):195-204. <https://doi.org/10.1002/jctb.280430305>.
- Espiari Sh., Rashchi F. and Sadrnezhad S.K. (2006): Hydrometallurgical treatment of tailings with high zinc content. Hydrometallurgy, 82, pp 54–62. <https://doi.org/10.1016/j.hydromet.2006.01.005>.
- Feng, Q., Wen, S., Deng, J., & Zhao, W. (2017): Combined DFT and XPS investigation of enhanced adsorption of sulfide species onto cerussite by surface modification with chloride. Applied Surface Science, 425, 8-15. <https://doi.org/10.1016/j.apsusc.2017.07.017>.
- Feng, Q., Zhao, W., & Wen, S. (2018): Surface modification of malachite with ethanediamine and its effect on sulfidization flotation. Applied Surface Science, 436, 823-831. <https://doi.org/10.1016/j.apsusc.2017.12.113>.
- Habbache N, Alane N, Djerad S, Tifouti L. (2009): Leaching of copper oxide with different acid solutions. Chemical Engineering Journal. 15;152(2-3):503-8. <https://doi.org/10.1016/j.cej.2009.05.020>.
- Haghighi, H.K.; Moradkhani, D.; Sedaghat, B.; Najafabadi, M.R.; Behnamfard, A. (2013): Production of copper cathode from oxidized copper ores by acidic leaching and two-step precipitation followed by electrowinning. Hydrometallurgy, 133, 111–117. <https://doi.org/10.1016/j.hydromet.2012.12.004>.
- Han G, Wen S, Wang H, Feng Q. (2021): Surface sulfidization mechanism of cuprite and its response to xanthate adsorption and flotation performance. Minerals Engineering. 1; 169:106982 <https://doi.org/10.1016/j.mineng.2021.106982>.
- Han, J.W.; Xiao, J.; Qin, W.Q.; Chen, D.X.; Liu, W. (2017): Copper Recovery from Yulong Complex Copper Oxide Ore by Flotation and Magnetic Separation. The Journal of The Minerals, Metals & Materials Society. 69, 1563–1569. <https://doi.org/10.1007/s11837-017-2383-x>.
- Künkül A, Gülezgin A, Demirkiran N. (2013): Investigation of the use of ammonium acetate as an alternative lixiviant in the leaching of malachite ore. Chemical Industry and Chemical Engineering Quarterly/CICEQ. 19(1):25-35. <https://doi.org/10.2298/CICEQ120113039K>.
- Li, Y., Wang, B., Xiao, Q., Lartey, C., & Zhang, Q. (2017): The mechanisms of improved chalcopyrite leaching due to mechanical activation. Hydrometallurgy, 173, 149-155. <https://doi.org/10.1016/j.hydromet.2017.08.014>.
- Liu, M., Wen, J., Tan, G., Liu, G., & Wu, B. (2016): Experimental studies and pilot plant tests for acid leaching of low-grade copper oxide ores at the Tuwu Copper Mine. Hydrometallurgy, 165, 227-232. <https://doi.org/10.1016/j.hydromet.2016.04.009>.
- Mao YB, Deng JS, Wen SM, Fang JJ, Yin Q. (2016): Recovering copper from volcanic ASH by NH<sub>3</sub>·H<sub>2</sub>O–NH<sub>2</sub>COONH<sub>4</sub>. Russian Journal of Non-Ferrous Metals. 57(6): 533-43. <https://doi.org/10.3103/S1067821216060158>.

- Naguman PN. (2008): The chemistry and kinetics of oxidized copper sulfiding by sodium thiosulfate. *Russian Journal of Non-Ferrous Metals*. 49(6):433-7. <https://doi.org/10.1016/j.hydromet.2017.02.024>.
- Rucker, D.F.; Zaebs, R.J.; Gillis, J.; Cain, C., IV; Teague, B. (2017): Drawing down the remaining copper inventory in a leach pad by way of subsurface leaching. *Hydrometallurgy*. 169, 382–392. <https://doi.org/10.1016/j.hydromet.2017.02.024>.
- Shabani MA, Irannajad M, Azadmehr AR. (2012): Investigation on leaching of malachite by citric acid. *International Journal of Minerals, Metallurgy, and Materials*. 19(9):782-6. <https://doi.org/10.1007/s12613-012-0628-9>.
- Shayestehfar MR, Nasab SK, Mohammadalizadeh H. (2008): Mineralogy, petrology, and chemistry studies to evaluate oxide copper ores for heap leaching in Sarcheshmeh copper mine, Kerman, Iran. *Journal of hazardous materials*. 15;154(1-3):602-12. <https://doi.org/10.1016/j.jhazmat.2007.10.100>.
- Tanda BC, Eksteen JJ, Oraby EA. (2017): An investigation into the leaching behaviour of copper oxide minerals in aqueous alkaline glycine solutions. *Hydrometallurgy*. 1;167:153-62. <https://doi.org/10.1016/j.hydromet.2016.11.011>
- Turan, M.; Arslanoglu, H.; Altundogan, H.S. (2015): Optimization of the leaching conditions of chalcopyrite concentrate using ammonium persulfate in an autoclave system. *J. Journal of the Taiwan Institute of Chemical Engineers*. 50, 49–55. <https://doi.org/10.1016/j.jtice.2014.12.009>.
- Wang, G. R., Liu, Y. Y., Tong, L. L., Jin, Z. N., Chen, G. B., & Yang, H. Y. (2019): Effect of temperature on leaching behavior of copper minerals with different occurrence states in complex copper oxide ores. *Transactions of Nonferrous Metals Society of China*, 29(10), 2192-2201. [https://doi.org/10.1016/S1003-6326\(19\)65125-3](https://doi.org/10.1016/S1003-6326(19)65125-3).
- Wei LI, Tang MT, Tang CB, Jing HE, Yang SH, Yang JG. (2010): Dissolution kinetics of low grade complex copper ore in ammonia-ammonium chloride solution. *Transactions of Nonferrous Metals Society of China*. 1;20(5):910-7. [https://doi.org/10.1016/S1003-6326\(09\)60235-1](https://doi.org/10.1016/S1003-6326(09)60235-1).
- Wu D, Wen S, Yang J, Deng J, Jiang L. (2013): Dissolution kinetics of malachite as an alternative copper source with an organic leach reagent. *Journal of Chemical Engineering of Japan*. 20;46(10):677-82. <https://doi.org/10.1252/jcej.13we035>.
- Yoshida T. (2003): Leaching of zinc oxide in acidic solution. *Materials Transactions*, 44 (12), pp 2489–2493. <https://doi.org/10.2320/matertrans.44.2489>.

## SAŽETAK

### Kinetika otapanja uzorka rude bakrenog oksida i optimizacija parametara utjecaja pomoću metodologije odzivne površine

U radu se istražuje izluživanje uzorka rude bakrenog oksida iz rudnika bakra Qaleh-Zari s vrlo visokim udjelom Cu od 5,4% (malahit i azurit), kako bi se procijenili utjecaji značajnih parametara na stupanj iskorištenja rude, uključujući koncentraciju sumporne kiseline, sadržaj čvrstog, veličinu čestica i brzinu miješanja. Zatim su korišteni metodologija odzivne površine (eng. RSM) i centralno kompozitni plan (eng. CCD) za optimizaciju procesa izluživanja i procjenu međudjelovanja parametara. Kako bi se dodatno analiziralo izluživanje, proučavana je kinetika otapanja bakra na temelju modela jezgre (eng. SCM). Rezultati su pokazali smanjenje iskorištenja rude s povećanjem udjela čvrstih čestica i/ili veličine čestica. Nasuprot tome, utvrđeno je da svako povećanje brzine miješanja i/ili koncentracije kiseline povećava iskorištenje. Zanimljivo je da povećanje sadržaja sumporne kiseline iznad određene razine nije imalo značajan učinak na iskorištenje. Optimalno izluživanje bakra dobiveno je s udjelom čestica 25,12%, brzinom agitacije 586 okretaja u minuti, veličinom čestica 70  $\mu\text{m}$  i koncentracijom sumporne kiseline od 12,5%. Ispitivanje kinetike izluživanja pokazuje da je brzina otapanja kontrolirana difuzijom tekućine prema modelu slojeva uz energiju aktivacije 30,71 kJ/mol.

#### Ključne riječi:

bakreni oksid; izluživanje; kinetika; metodologija odzivne površine; optimizacija.

#### Author's contribution

**Hassan Maleki** (1) (MSc Student of Mineral Processing) performed tests, analyses, provided reports and wrote the article. **Sajjad Chehrehgani** (2) (Associate Professor of Minerals Processing) proposed the idea, provided technical suggestions and guided the research. **Mohammad Noaparast** (3) (Full Professor of Mineral Processing) proposed the idea, provided technical suggestions and guided the research. **Mir Saleh Mirmohammadi** (4) (Assistant Professor of Mineral Exploration) performed mineralogical studies. **Minoo Ghanbarzad** (5) (MSc of Economic Geology) measured copper grade with the atomic absorption technique and provided the samples.